# Three-Dimensional Optimization of Touch Panel Design with Combinatorial Group Theory

by

Christie Kong

A thesis
presented to the University of Waterloo
in fulfillment of the
thesis requirement for the degree of
Master of Applied Science
in
Management Sciences

Waterloo, Ontario, Canada, 2010

I hereby declare that I am the sole author of this thesis. This is a true copy of the thesis, including any required final revisions, as accepted by my examiners.

I understand that my thesis may be made electronically available to the public.

**Abstract**

This thesis documents the optimized design of a touch screen using infrared technology as a three dimensional problem. The framework is fundamentally built on laser diode technology and introduces mirrors for signal reflection. The rising popularity of touch screens are credited to the naturally intuitive control of display interfaces, extensive data presentation, and the improved manufacturing process of various touch screen implementations. Considering the demands on touch screen technology, the design for a large scaled touch panel is inevitable, and signal reduction techniques become a necessity to facilitate signal processing and accurate touch detection. The developed research model seeks to capture realistic touch screen design limitations to create a deployable configuration. The motivation of the problem stems from the significant reduction of representation achieved by combinatorial group theory. The research model is of difficulty NP-complete. Additional exclusive-or functions for uniqueness, strengthening model search space, symmetry eliminating constraints, and implementation constraints are incorporated for enhanced performance. The computational results and analysis of objectives, valuing the emphasis on diodes and layers are evaluated. The evaluation of trade-off between diodes and layers is also investigated.

**Acknowledgements**

For my supervisor, Professor Pin-Han Ho, I reserve the deepest of gratitude as he fostered my research and educational progression. It was his inspirational energy and motivational direction that saw to the cultivation of my thesis.

I would like to thank the perspective feedback from my readers Professor Benny Mantin and Professor Zhou Wang.

As always, I give thanks to: my sister for being my better half; Lina for the endless espresso; Tariq, Jaimal, and Dan for making this a quest; Bissan and Elspeth for their company; as well as, Thomas and Stephen for encouraging new project ventures. I offer my regards to all my friends who have supported and enlightened me.

James, my hero and fortune.

While the destination will be rewarding, the journey itself has been more than fulfilling.

*For my loving parents, who gave me values, courage, and always a cup of hot tea.*

# Contents

# List of Tables

# List of Figures

# Chapter 1

# Introduction

The last technological revolution, the information era, contributed to the overabundance of available data in the current generation. Modern society struggles to interact with the volume of information in manageable quantities. The recent innovation of touch screen technology in mainstream applications has received acclaimed success in easing user interactions with data. The widely popular implementations of touch screens on personal handheld and mobile smartphones have redefined consumer expectations. The control of onscreen tasks is naturally intuitive and removes the traditional mouse and keyboard as limited input methods. In the industry of electronic devices, a successfully integrated touch screen can gain control of a dominant market share. The Apple iPhone, which was first launched in January 2007, had reintroduced the general public to the touch screen interface, which incorporated seamless application inputs and multi-touch control. While the concept of touch screen is not revolutionary, the responsiveness and versatility of onscreen control available in existing mobile units far exceed the performance of previous productions. The enhancements are primarily attributed to the technological advances of manufacturing processes, engineering design considerations, and user interaction with software interfaces.

## 1.1 Touch Screen Technology Issues

The majority of touch screen technology implementations are limited to small surfaces due to the computationally intensive and costly hardware equipment. Expanding existing touch screen technology beyond the design capacity is suboptimal as the technology proves

limiting in supporting responsive touch detection, equipment costs, and redundant signal processing. Using existing technology and methods, the creation of a large dimension touch screen panel would be infeasible for mass consumer markets. Although existing technologies have been successfully introduced for small panel operation, the same methods of implementation cannot be applied on large scaled panels. The current market trends for touch panels are found on mobile devices, retail registers, computer displays, and computer tabletop but rarely an entire wall panel. For larger panel dimensions, the same performance demands on responsiveness and accuracy of touch detection is expected to be relatively similar to smaller panel resolutions. However, as the larger touch panel requires increased sensor and receiver data for each additional resolution line to ensure the precise level of pixel clarity and accuracy, using existing methods of implementation would compromise the overall performance of the touch panel.

Even at smaller dimensions, the one signal detection for every one pixel of horizontal and vertical resolution defined by the panel can severely undermine the performance of the touch screen panel. As the dimension of the panel increases, so does the linear relationship of equipment resources. The additional equipment and computational overhead does not justify an inefficient and obsolete design framework. Hence, it is expected that the demanded touch screen dimension and performance in the near future far exceeds the capabilities of current methodology.

## 1.2 Thesis Contributions

The main contribution of this thesis is the design and implementation of a linear integer programming formulation that models the configuration of electronic components to optimize the design of a touch panel within a three dimensional space. The thesis goal is to incorporate information theory reduction techniques, combinatorial group theory, and superimposed codes to model the electrical engineering design constraints of an optimized touch panel that can be transferred into an applied solution. The beneficial reduction achieved through combinatorial group theory and superimposed codes from coding theory are applied in the structural design formulation. The uniqueness constraint from combinatorial group theory is implemented and evaluated in three approaches, namely, the built-in CPLEX function, linear, and array formulations. The model is strengthened and

symmetry eliminating constraints are added to tighten the entire solution search space. The difficulty of modeling varying matrix dimensions are overcome by a set of CPLEX implementation constraints. The influencing restriction on the number of diodes and layers assigned are investigated, as well as the tradeoff between the two to provide a deeper understanding into the nature of the problem. The results acquired through extensive simulations are evaluated, and serve as a foundation for understanding the relationship of the design model. The research model evaluates the application of infrared touch screen technology, and considers transmitted signals at right angle reflections, with results evaluated for future work. The model proposed is a novel approach in overcoming the limitations of touch screen technology issues, and investigates a preliminary solution methodology for large-scale touch panels using existing technology.

The thesis is organized as follows. Chapter 2 provides a background on the existing touch screen technologies, multi-touch invention, as well as the foundation of the mathematical information behind combinatorial group theory and superimposed codes. In Chapter 3, the entire model formulation is derived considering the methods in the previous chapter. The results of the model formulation are presented and evaluated in Chapter 4. Finally, Chapter 5 provides conclusive remarks which summarize the contributions of this research topic.

# Chapter 2

# Background

Touch screen technology have existed since the early 1960s with many performance limitations. However, due to modern manufacturing and technology design advancements, the seamless integration of touch screen panels on small mobile devices have gained popularity mainly from the intuitive user interface. The interaction with an application through direct touch of graphical elements is a more natural approach that results in improved efficiency and accuracy [1]. In this chapter, the touch screen technology market and existing implementation methods are explained. A brief overview of multi-touch and components of the model design technology are also covered. The motivational mathematical reduction achieved by combinatorial group theory and superimposed codes methods are introduced.

## 2.1 Touch Screen Technology

The enhancements on modern manufacturing processes and engineering designs have facilitated the emergence of touch screens. A prevalent usage of touch screen technologies exist in conference rooms, educational classrooms, transportation schedules, financial institutions, simulation control rooms, staging, retail signage, and indoor venues. In 2013, the demand for public displays of touch modules and signage is expected to reach a forecast of 5.4 million units sold and a market segment worth $2.9 billion [2] according to an industry study completed in 2009.

In 1963, Ivan Sutherland demonstrated the Sketchpad, the first interactive graphical user interface using a light pen to manipulate drawings comprised with physical knobs,

push-buttons, and toggle switches [3]. Then in 1967, Douglas Engelbart introduced the two keyboards (alphabets and functional key cluster) and mouse [4]. Apple Macintosh popularized the use of special purpose keys with on screen graphical user interface widgets that have become widely accepted on desktop computers since the early 1980s. Recently, Apple has again revolutionized the multi-touch input screens on their iPhone and iPad product lines. The advantage of increasing the amount of information available over flat panel touch displays through user interface has been adapted predominantly in the automotive, retail cash register, mobile device, and the aerospace industries [5]. The use of touch screens prevail on handheld computing devices such as mobile phones, personal digital assistant (PDA), digital cameras, and music players, where display space is restrictive [6].

Typically, a touch screen is comprised of a touch panel, a controller and a software driver. The clear touch panel is a touch sensitive surface that is positioned directly in front of the viewable area on a display screen with a graphical user interface. Touch events are registered and signals are sent to the controller to process the data to the computer system. The software driver then translates the received touch input events into the corresponding computer events. The main commercial implementation of touch screen technology are resistive, surface acoustic wave (SAW), infrared, optical imaging, and capacitive. All of the existing current implementation of touch screen technologies require at least one sensor and one receiver pair to send horizontal and vertical coordinates to a processor controller for localization of the signal. The design implementation requires that every resolution line is a unique input sensor on the screen and no signal reduction is attempted.

### 2.1.1 Resistive Touch Screen Technology

A resistive touch screen is a glass, polyester, or acrylic panel coated with electrically conductive as well as resistive layers. The thin electrically conductive layers are separated by small insulating spacers. A current flows on the screen. The touch is localized when the force closes the insulator spacer gap, causing the two layers to conduct electricity. When it touches the resistive layer, the closing switch registers the change in voltage, which defines the location of the touch.

Resistive touch technology is affordable compared to other methods technologies; how-

ever, the light quality of screen transmission is diminished by 30-20% [6], [7] and pressure sensitivity limits the speed of registering touch detection. Most applications of resistive touch screen technology are found in harsh environments typically used in control and automation systems.

### 2.1.2 Surface Acoustic Wave Technology

SAW technologies, one of the most advanced touch screen technology, uses two transducers for transmitting and receiving along the horizontal and vertical axis of the touch panel. The glass acts as a reflector in SAW touch screens. The controller sends a signal to the transmitting transducer, which converts the signal into an ultrasonic wave and emits it to the reflectors along the edges of the panel. The ultrasonic wave is refracted until it reaches the receiving transducer when the wave is converted back into an electrical signal to the controller. When a touch is applied to the panel, the acoustic energy of the waves is absorbed and sensors located across from the source of the waves detect this change and sends the information to the controller for processing. In comparison to resistive and capacitive technologies, SAW touch screens have a superior image clarity, better resolutions and higher transmission of light. However, the surface of SAW technology is subjected to the interference of dirt, dust, and environmental fluctuations.

### 2.1.3 Infrared Touch Screen Technology

Infrared technologies rely on light beams, such as laser emitting diodes, sent horizontally and vertically over the panel. When the panel is touched, the light paths of the emitting diodes are interrupted and light detectors across the light emitting diodes sense the interruption allowing the controller to process the location of the touch. Without patterning the glass surface, infrared touch screens are more durable and are optically clear in comparison to resistive and capacitive touch screens. The use of light beams can be resized for various dimensions of the desired panel.

One adaption is the implementation of frustrated total internal reflection (FTIR). Introduced in 2005, this methodology allows for multi-touch tracking and the name of the technology refers to an optical phenomena [8]. Total internal reflection occurs when a ray of

light enters a medium at an angle larger than the critical angle with respect to the normal of the surface. The exact angle depends on the refractive indices of both materials and the critical angle is determined using Snell's Law. If the refractive index were lower, the light would not pass through and all the light is reflected. Since the angle of incidence is greater than the critical angle such that the ray is closer to being parallel to the boundary, the light does not pass through and all of the light is internally reflected. By flooding a piece of acrylic with infrared light, the light rays are trapped to bounce within the acrylic by total internal reflection. When a touch occurs at the surface, the light rays are identified as frustrated as the light cannot pass though into the contact material and the reflection is lost. An infrared camera is installed beneath the acrylic panel and faces the user input to capture the contact points by the frustrated light rays. Generally, FTIR is used for detecting finger touches by using standard web cameras that are sensitive towards infrared lights. An FTIR system can acquire touch blobs at high spatial and temporal resolutions, with the additional benefit of very large scalable installations.

### 2.1.4 Optical Sensing Touch Screen Technology

Optical sensing is a recent development. It relies on the use of two or more image sensors placed at the corners of the screen and an infrared backlight to be placed at the camera's field of view on an opposing screen. Using the shadow of the touch, the image sensors triangulate the location and measures the visual hull of the touching object. Although this implementation is computationally intensive and requires costly equipment, it has begun to gain popularity due to the system's versatility and scalability in execution.

Successful optical sensing touch screen has been implemented in MetaDesk [9], HoloWall [10], and Designer's Outpost [11] frameworks using video cameras and computer vision techniques to compute a touchable image. The aforementioned systems creates a simultaneous video projection, and facilitates surface sensing through the use of a diffusing screen material from the camera view, which only resolves objects either on or very near the surface. The touch image was produced by cameras systems that revealed the appearance of the object as if it were viewed from behind the surface. Application events can be triggered by using image processing techniques on the touch image. The implementation and computation of such a system is extensive in rendering graphics.

### 2.1.5 Capacitive Touch Screen Technology

On a capacitive overlay, the glass panel is coated with a thin coating of charge storing material. A capacitive touch screen can be classified as either a surface or projected capacitance. In a surface capacitance, the insulator is coated on one side by a conductive layer. The small voltage applied to the layer results in a uniform electrostatic field and when a conductor touches the uncoated surface, a capacitor is created. When a conductive touch is applied on the surface capacitance screen with a charge drawn at the point of contact, the circuits located at the corner of the screen measures the fluctuation in capacitance and current flow that changes proportionally based on the relative distance from the circuitry location. Although this method is durable, it is prone to false location identification due to the effects of parasitic capacitive coupling and requires calibration to remain sensitive. In projected capacitance technology, a coordinate system is etched into two separate perpendicular layers of conductive materials that allows for more accurate and flexible operations. The advantage of projected capacitance is the enhanced resolution of detection. The conducting layers can be coated with protective insulating layers and still perform optimally, unlike resistive technology. Projected capacitance touch technology can be implemented using either self capacitance or mutual capacitance. In general, capacitive touch screens are considered to be very durable and have high clarity. The implementation of capacitive touch screens has gained popularity in smartphones and mobile devices. The transparent screen is often implemented using indium tin oxide (ITO) as the conductive medium. The touch screen may include a plurality of capacitance sensing nodes that are either self or mutual capacitance. Both types of capacitance measurements can operate independently of other nodes such that simultaneous occurring signal representatives of various points on the touch panel are made.

In self capacitance, a single electrode can be measured relative to ground. The sensing arrangement is patterned into spatially separated electrodes and traces such that each represents a different coordinate, and the traces join with the electrodes forming a capacitive sensing circuit. Usually, the arrangements are implemented using the Cartesian coordinate system ($x$ and $y$ axis) such that the electrodes create a grid array with each electrode representing a unique $x$-$y$ coordinate. In operation, the capacitive sensing circuitry monitors the fluctuation in capacitance at each electrode and multiple touches are determined by the magnitude of changes. A finger on the surface of the touch panel would draw charge within close proximity to the electrode and affects the measured capacitance value.

In the case of mutual capacitance, the measurement occurs between at least a first and second electrode. The sensing arrangement is now patterned into a grouping of spatially separated lines formed on two distinct layers. On the first layer, driving lines are separated from the second layer of sensing lines. Although the layers partition the separation, sensing lines traverse, intersect, or cut across the driving lines to form a capacitive coupling node. The behaviour of the sensing line cut across the driving lines depends on the coordinate system used. In a Cartesian coordinate system, the sensing lines exist perpendicular to the driving lines, forming nodes at distinct $x$ and $y$ coordinates. On the contrary, another common polar coordinate system arranges the sensing lines in concentric circles, with the driving lines extending outward in radial lines. A voltage source is connected to the driving lines and a capacitive sensing circuit is connected to the sensing lines. In operation, a current is driven through one driving line at a time due to capacitive coupling, carrying the current to the sensing line at each node. The sensing circuitry monitors the change in capacitance at each node. The magnitude and position is conveyed to identify multiple touch events. Again, a capacitive coupling node can identify a finger at close proximity as the drawn charge affects the measured capacitance.

A simplified diagram of mutual capacitance circuitry is illustrated in Fig. 2.1. At the location of the touch, a capacitive coupling node is formed from the spatial separation of the driving line before the touch, and a sensing line after the touch location. A voltage source is electrically coupled to the driving line and a capacitive sensing circuitry is coupled to the sensing line. Both the driving line and sensing line have been configured to carry a current to the capacitive sensing circuitry. A filter can be installed on the sensing line to eliminate parasitic capacitance, which is a result of the large surface area of lines from the rows and columns relative to other lines. The filter rejects the stray capacitance effects to present a clean representation of charge transferred across the touch location [12]. When the screen is void of touch, the capacitive coupling at the node remains fairly constant. However, when an object like a finger comes into proximity of the node, the capacitive coupling changes as the finger effectively shunts the field such that the charge projected across the touch location is reduced. With this measured change in current, the position is reported in raw data form to be processed on the host controller. The capacitance sensing circuit performs this analysis at each node simultaneously to enable multipoint sensing.

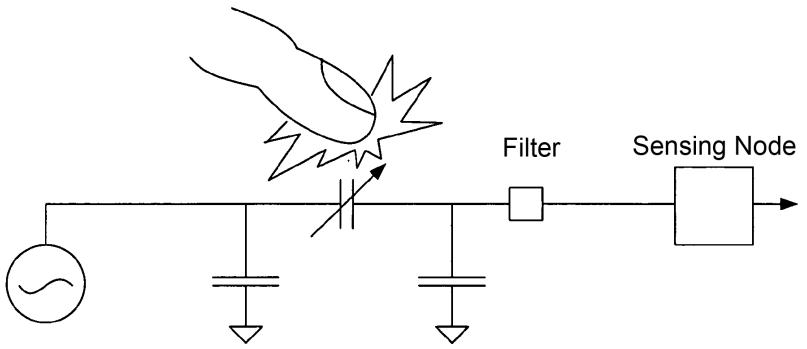


Figure 2.1: Touch Screen Mutual Capacitance [12]

Apple integrated capacitive touch sensing technology into a liquid crystal display (LCD) [13]. The basic structure of an LCD is comprised of a top glass, a liquid crystal and a bottom glass layer. Both the top and bottom glass layers can be patterned as the boundaries of the cells to contain the liquid crystal for a display pixel. Alternatively, the top and bottom glass planes can be patterned with various layers of conducting materials and thin film transistors, permitting the voltage across the liquid crystal cells to be varied. This variation allows for the manipulation of the liquid crystal orientation, allowing control of color and brightness of each pixel. The benefits of the integration eliminates redundant structures or layers, which reduces manufacturing process, cost, and overall thickness of the touch screen LCD. The manufacturing of LCD panels uses batch processing on large pieces of glass known as mother-glass. Two pieces of mother-glass are required; one top piece is used to provide the substrate for the colour filter, black matrix, and the upper electrode, and another bottom piece of mother-glass is used for the substrate of the active matrix array and the drive circuitry [13]. The two mother-glasses are aligned, then pressed together and finally heated to seal the glass pieces, producing a durable panel structure. The individual panels can have the edges grounded before filling the liquid crystal, which are then sealed again. Polarizers, flexible printed circuitry, and electrical components can be attached to the panel substrate or at the end of the manufacturing process.

The integration of capacitive touch sensing technology into an LCD screen can be achieved by introducing touch sensing circuitry on the top and bottom glass. Towards the user side, the top of the glass can be deposited with touch sensing electrodes while

the underside of the top glass will be patterned with touch drive electrodes. A stack up diagram of a combined LCD with capacitive sensing technology is shown in Fig 2.2. An additional hard-coated PMMA layer is used to protect the LCD polarizer. Additionally, the top glass and a second polarizer is used between the bottom glass and the backlight. The conductive dots within the panel are connected to the drive electrodes to the driver on the bottom glass. It is also possible to add touch sensing elements outside the liquid crystal module.

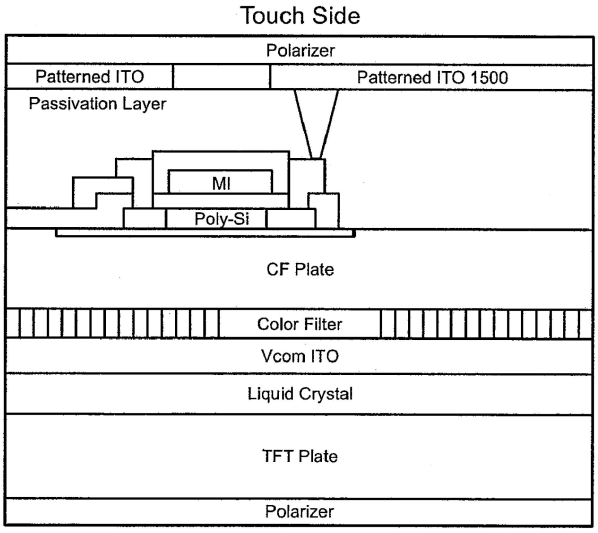


Figure 2.2: Stack Up Diagram of LCD Capacitive and Multi-Touch Screen [13]

## 2.2 Integration of Multi-Touch

Multi-touch flourished as a research area in the mid 1980s. In 1985, a multi-touch tablet surface with front projections was demonstrated with the capability of sensing pressure and location of multiple touch points by using capacitive measurements [14]. DiamondTouch used capacitive coupling to track the inputs of four different individual's control in 2001 [15]. SmartSkin used the signals of an antenna grid to reference the distortion created by finger touch in 2002 [16]. ThinSight used infrared sensors behind the laptop display to track multiple finger touches in 2007 [17].

Early touch screen devices were slow to register touch detection and were limited to

single touch registration for resistive, capacitive, SAW, and infrared touch screens. Even when multiple points were placed on the sensing surface, the touch screen was only capable of recognizing a single detection. The average of all simultaneous multiple touch points are used to determine a single point as reported to the processor in resistive and capacitive touch screens. Multiple inputs on resistive, capacitive, SAW and infrared touch screens thus previously yielded faulty results.

With the introduction of the iPhone, Apple capitalized on the development of multi-touch control implemented with capacitive sensing touch screen technology. The invention was able to track multiple points of contact simultaneously and the changes in touch gestures would register control actions carried out by the mobile device [18]. A mutual capacitive touch screen that supports multi-touch will require a series of layers having independent drive and sense electrodes separated by a non-conducting glass layer. The method of execution was able to separately distinguish the multiple touches and reported multiple touch data. The touch screen itself was partitioned into independent and spatially distinct sensing points throughout the plane, such that each individual touch point was capable of generating a signal concurrently. This required the active driving of several sensing points, and analysis of all sensing line outputs connected to the sensing points. An additional phase in comparison to traditional touch screen technologies was created to produce and analyze an image produced on the touch panel from sequential time frames, such that the evaluation can determine the change in gestures. Hence, the digital signal processing method had to incorporate the reception of raw data, which included the values for each transparent capacitive sensing node and filtration, to generate a gradient of data to calculate the boundaries for touch regions. Each touch region had corresponding coordinates. Apple's multi-touch technology can track fifteen touch points, allowing all ten fingers, two palms and three other signals [12]. The drive sensing points on the panel would be interrupted by a touch and thus cause a resulting output from the sensing points to be read. The information would be sent for analysis to compare current data with the previous data date to perform the appropriate action based on the comparisons in [18], [13].

## 2.3 Chosen Research Framework Approach and Components Technology

The research in this thesis seeks to determine a display arrangement for large-scale transparent touch panels using existing technologies. The implementation of available components that allowed flexibility in design arrangement suitable for optimization was the infrared laser diode touch screen technology. The advantages of infrared technologies are the availability of equipment and ability to support design scalability.

By using the components of laser diodes, mirrors, and receivers, the design model framework attempts to optimize the arrangement for minimized cost without compromising operation performance. A laser diode is most commonly formed from a p-n junction and powered by electric current. The coherence, monochromaticity, and collimation properties of light from a laser diode enables the laser light to stay as a tight confined beam over large distances [19]. Manipulated properties of the laser beam are temporal change, such as switching or pulse slicing, spatial energy intensity distribution change, directional change by refraction or waveguides, total intensity power or energy change, frequency or phase change, and polarization change [20]. The mirrors have a reflective nature that is controlled entirely by the angle of incidence. The receiver in this model is light sensitive to determine interruption by a touch. In this thesis, the flexibility of component properties are not fully evaluated in the research model. The research model of interest focuses on gaining insight into the overall design to take advantage of the technology flexibility of the components.

## 2.4 Combinatorial Group Testing Method

During World War II when resources were scarce for the screening of syphilis, Robert Dorfman proposed the idea of group testing [21]. Instead of conducting individual sample testing on a large population of people for which contained a small set of contaminates, using a systematic combination of group testing would indicate the exact contaminate with a significantly reduced set of tests. The general group testing problem is defined by a large population of items containing a small set of defectives that require efficient identification. Items are either defectives or working properly.

Group testing algorithms can be divided into either Combinatorial Group Testing (CGT) or Probabilistic Group Testing (PGT). In CGT applications, it is often assumed that the number of contaminates among all items is equal to or at most a fixed positive integer, whereas for PGT, the probability of a contaminate occurring is fixed at a desired value. When the pool is simultaneously tested $s$ times, where subsequent test pools are collected based upon previous results, then the CGT algorithm is said to be an $s$-stage algorithm. Group testing strategies can be either adaptive or non-adaptive. When testing is adaptive, each test is specified based on the previous test outcomes. If all tests are specified without prior knowledge of the outcomes of other tests, then the testing algorithm is non-adaptive, which is equivalent to being 1-stage. A group testing algorithm can also be characterized by error tolerance if it can detect or correct errors found in test outcomes through the use of Hamming distance [22], [23].

CGT has been applied in the study of quality control in product testing [24], file storage systems [36], experimental variable screening [26], conflict resolution algorithms for effective multiple-access channels [27], [28], data compression [29], computation of statistics for data stream model [30], [31], and testing concentration of chemical and pathogenic contaminants [32]. Recently, CGT has been successfully applied in the study of computational molecular biology. The model applies to the screening of library clones using hybridization probes [33], and in the sequencing of hybridization [34].

In the application of touch screen panels, for a single touch, the detection would cause an interruption of a diode sensor amongst the numerous uninterrupted sensors in a non-adaptive testing strategy. The three basic problems in CGT, whether the matrix is $d$-separable, $\bar{d}$-separable or $d$-disjoint, are all known to be NP-complete [35], where $d$ is the column. Hence, the diode path assignment and arrangement problem proposed is also of difficulty order NP-complete.

Let $S$ be the sample space of a group testing problem, then $M(S)$ be the minimax algorithm for $S$, resulting in the well known information theory bound [21].

$$M(S) \geq \lfloor \log_2 |S| \rfloor + 1 \tag{2.1}$$

## 2.5 Superimposed Coding

Kautz and Singleton in 1964 first studied superimposed codes in the application for file retrieval, data communication, and magnetic memory design [36]. They defined a binary superimposed code as a set of codewords whose digit-by-digit Boolean sums have a distinguished quality. In combinatorial science, superimposed codes have been used in group testing [47], [38], perfect hash families [39], key storage in secure network [40], [41], and tracing decoded data transmission traitors [42]. Lately, new bounds on a generalized form of superimposed codes have been found using optimal algorithms [43]. Depending on the application, several code families exist for the creation of the principal code parameters to be based upon such as $q$-ary conventional error-correcting codes, combinatorial arrangements used in block designs and Latin squares, graphical construction, and parity check matrices using standard binary error correction codes. The two main problems in superimposed codes is to either minimize the length of codewords given cardinality of distinguishability, or find the maximum cardinality of distinguishability for a given code word length. The main problem defined by a strength of $w = r = 1$ constitutes the famous Sperner theorem, which has been completely proved in [44].

The fundamental similarity of non-adaptive CGT algorithms and superimposed codes is the identical matrix representation structure for which the constraints are imposed upon. The main incentive for the model formulation to apply superimposed coding structure is the uniquely identifiable quality of code designs, which removes the decoding or deciphering of codes assigned to diodes for touch localization that would otherwise contribute to increased computational overhead.

# Chapter 3

# Model Formulation

In an accurate and viable solution, the touch screen design linear model must account for placement of diodes and mirrors as feasible within the allocated frame space at the edges of the panel to facilitate design arrangements. The motivation in the approach described herein is based on CGT, which utilizes a significant reduction of independent signals to represent a substantial group. The use of a single laser diode and receiver pair to sense each resolution line of pixel grows linearly in relation to the touch screen panel dimension. While it is sufficient at smaller dimensions, the design of a large-scale panel size will involve cumbersome calculations for each sensor and the touch panel will lag due to the overhead expense for each pair of sensors, making large-scale touch panels unrealistic to achieve using existing technology. However, when implementing the methods of CGT, the model must arrange laser diodes, receivers, and mirrors while considering the desired design limitations in the depth, equipment trade-off, and functional attributes of the touch panel.

The difficulty of this problem stems not only from the arrangement of mirror and diode placement, but also the evaluation of optimal configurations based on permutation possibilities. It is possible to implement the problem in a two stage solution process by first finding the optimal paths traversed by diodes. Then, the problem is resolved with the solidified paths traversed while minimizing the considered cost objectives. However, this implementation was not further investigated due to the concern of locally optimal results and its failure to fully represent the problem.

## 3.1 Linear Model Preliminaries

A mathematical programming problem is a class of decision problem focused on the efficient use of limited resources to achieve a desired objective. Where $f(X)$ is the objective function and $g_i(X)$ are the constraints, the mathematical problem is given by:

$$\begin{aligned} &\text{Max } f(X) \\ &\text{subject to} \qquad g_i(X) \leq 0 \qquad \forall i = 1, 2 \ldots m. \qquad (3.1) \\ &\qquad\qquad\quad X \geq 0 \qquad (3.2) \end{aligned}$$

where $X = (x_1, x_2 \ldots x_n)^T \in R^n, i = 1, 2 \ldots \text{m}$ are real valued functions of $X$.

When the functions $f(x)$ and $g(x)$ are both linear with the presence of linear equality and/or inequality constraints, the model becomes a linear programming problem. The applications of linear programming models are popular in military, industrial, governmental, and mathematical science since the development of the simplex method by George B. Dantzig in 1947 [45]. The extensive use of linear programming can be attributed to the intrinsic ability of modeling complex and large problems using effective algorithms and solvers to solve the problems within a reasonable amount of time. Since Karmarkar's projective interior point algorithm was introduced, a class of interior point methods have been devised that iteratively yields an exact optimal solution for solving linear programming problems in polynomial time procedures, which perform particularly favourable for general large-scale sparse problems [46].

## 3.2 Path Matrix Representation

Let $R_i$ and $C_j$ denote the row $i$ and column $j$ of a $t \times n$ binary element matrix $M$, where the set of column (row) indices correspond to '1'-entries. $M$ is identified as $d$-separable ($\bar{d}$ separable) if the Boolean sums or unions of $d$ columns (up to $d$ columns) are all distinct. For $M$ to be $d$-disjunct, the union of any $d$ columns cannot contain any other column, implying that the union of any up to $d$ columns will also be unique.

In the application of non-adaptive CGT algorithms and superimposed codes, a $t \times n$ $d$-separable matrix generates a non-adaptive $(d, n)$ algorithm with $t$ tests associating the columns as paths traversed and rows as diodes, and interpreting a 1-entry cell $(i, j)$ as a path traversed by that diode and zero as not. A set of $d$ columns will refer to a sample and the union of $d$ columns in a sample corresponds to the set of tests for which rows with an '1' entry in the union identifies a positive outcome signifying the touch interruption location. The $d$-separable property implies that each sample within $S(d, n)$ will generate a different set of tests with positive results. Hence, by matching the set of samples in $S(d, n)$ with positive tests, the localized touch detection can be determined.

A known upper bound on the number of defectives the problem is denoted by ($\bar{d}$, n) for which Hwang, Song and Du [47] proved that $M(\bar{d}, n)$ is at most one more than $M(d, n)$. Likewise, the $\bar{d}$-separable property makes the samples in $S(\bar{d}, n)$ distinguishable. A $t \times n$ $\bar{d}$-separable matrix generates a binary superimposed code with $n$ code words of length $t$ such that each supercode word are of the same length and transmitted. Since the exact code words are contained within the supercode word, the disjunct property makes each code uniquely identifiable and decodable without the use of deciphering techniques.

The focus of non-adaptive CGT algorithms are to minimize the number of tests $t$ for a given number of items $n$ and the motivation of superimposed codes are to maximize the number of code words $n$ for a given number of alphabets $t$. Both non-adaptive CGT algorithms and superimposed codes are actually two sides of the same problem, as both functions seek to maximize $d$ in the $\bar{d}$-separable and $d$-disjunct.

## 3.3 Matrix Variable Declaration

In the binary $A$ matrix, let the assignment of columns represent paths traversed and rows be diodes such that a value of '1' in $A(i, j)$ be the $i^{\text{th}}$ diode that traverses the $j^{\text{th}}$ path and '0' otherwise. The resolution of the touch screen panel is the variable $j$ and the variable $i$ determine the diodes assigned for a particular sample solution. The relationship between the $A$ matrix and assigned diode paths are illustrated in Figure 3.1. The assignment of diode one traverses the paths 1, 4, and 5 by the placement of mirrors on the right tracks of path 1, 4, and 5 as well as on the left tracks of path 4, and 5. The assignment of diode

two is placed on the right hand side of the panel and traverses the paths of 2 and 3 with mirrors placed accordingly. For both diode paths, the receiver is placed at the end of the right hand tracks on paths 3 and 5.

$$\text{Let } a_{ij} \text{ represent a binary variable } = \begin{cases} 1 & \text{if diode } i \text{ travels path } j \\ 0 & \text{otherwise.} \end{cases}$$

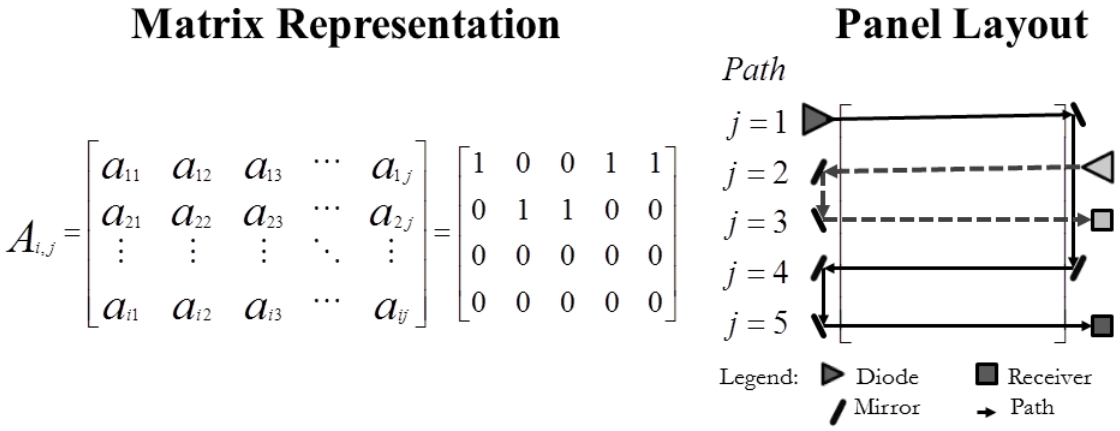


$$A_{i,j} = \begin{bmatrix} a_{11} & a_{12} & a_{13} & \cdots & a_{1j} \\ a_{21} & a_{22} & a_{23} & \cdots & a_{2j} \\ \vdots & \vdots & \vdots & \ddots & \vdots \\ a_{i1} & a_{i2} & a_{i3} & \cdots & a_{ij} \end{bmatrix} = \begin{bmatrix} 1 & 0 & 0 & 1 & 1 \\ 0 & 1 & 1 & 0 & 0 \\ 0 & 0 & 0 & 0 & 0 \\ 0 & 0 & 0 & 0 & 0 \end{bmatrix}$$

Figure 3.1: Diode arrangement matrix and panel layout for sample solution.

## 3.4 CGT Uniqueness Constraint Formulation

The implementation method requires that each code word be uniquely identifiable to successfully distinguish between each sensor and receiver pairs to localize touch detection without the additional usage of a lookup or decipher tables. To formulate the uniqueness constraint, all assigned diode to paths must be distinctive. This is achieved by the binary exclusive-or (XOR) operation. The logical operation XOR disjunction is only true for two operands of different binary values; the XOR truth table is shown in Table 3.1. To achieve uniqueness, all assigned possible path occupations must result in a binary XOR result of true or '1'. The XOR function is a non-linear function and must be converted for inclusion in our linear model formulation. The first method used the built-in XOR function in CPLEX. In the research model, two methods of representing the uniqueness constraint were implemented and the performance was evaluated.

Table 3.1: Exclusive-OR (XOR) truth table.

| $r = x \oplus y$ | $x$ | $y$ | $r$ |
|---|---|---|---|
| Case 1 | 0 | 0 | 0 |
| Case 2 | 1 | 1 | 0 |
| Case 3 | 0 | 1 | 1 |
| Case 4 | 1 | 0 | 1 |

### 3.4.1 Linear XOR Conditions

A linear equivalent of the XOR function can be represented by a set of four linear evaluations. Similarly, all of the equations must be satisfied for the XOR condition to be established and are added to the constraints of the linear model. In Case 1 from Table 3.1, when $x$ and $y$ are both zeros, Eq. (3.3)-(3.5) forces the result $r$ to be zero. In Case 2 for $x$ and $y$ are both ones, $r$ is bounded by Eq. (3.3), (3.4) and (3.6) to be zero. Case 3 is bounded by Eq. (3.3), (3.5), and (3.6) to a value of one; similarly, Case 4 is bounded by the combination of Eq. (3.4)-(3.6). This method uses simple linear operations.

$$r = x \oplus y$$

$$r \geq x - y \tag{3.3}$$

$$r \geq y - x \tag{3.4}$$

$$r \leq x + y \tag{3.5}$$

$$r \leq 2 - x - y \tag{3.6}$$

### 3.4.2 Array Operation of XOR

The uniqueness constraint can also be implemented as an array representation of XOR operation evaluation. This method was implemented in the investigation of transparent optical network failure localization achieved by monitoring trails in an integer linear program [48]. By defining four arrays within CPLEX programming and executing Eq. (3.7)-(3.10) such that it is always satisfied, the XOR operation is guaranteed to be successfully represented to ensure that each possible assignment paths remain uniquely distinguishable. Eq. (3.7) ensures that at least every assignment is unique. Eq. (3.8) performs an equality check while Eq. (3.9) is the equivalent of the binary AND operation. Eq. (3.10) is the definition

of the array $W$ as the element multiplication of array $a$ and array $b$.

$$\sum_{i=1} U_i \geq 1 \ \forall i \tag{3.7}$$

$$U[i] = a[i] + b[i] - 2W[i] \ \forall i \tag{3.8}$$

$$2W[i] \leq a[i] + b[i] \leq W[i] + 1 \ \forall i \tag{3.9}$$

$$\text{where } W[i] = a[i] * b[i] \ \forall i \tag{3.10}$$

## 3.5 Integer Linear Programming Model Constraints

In the design framework, a generated result must be applicable in implementation as defined by the electrical design limitations of the touch screen panel. To account for heat generation in diode operation, which can affect the precision of the laser beam, each touch panel is modeled by rows with sufficient spacing to a resolution line. Certain attributes limit the components (diode, mirror and receiver) in the framework. The diode light source is limited to horizontal transmission either from the left or right of the panel design. A mirror's light direction is limited by the right angle reflection from its source moving downwards or upwards based on the diode placement. A diode may only stream a singular path of light in one direction and cannot be split into two directions. A receiver must be placed at the end of a diode's path.

For example, when a light beam is transmitted from the first path to the third path, neither a mirror nor diode can be placed in the vertical vacancy in the second path as that would interrupt the light signal. However, it is possible to position a mirror in another track on the second path. A light beam from a vertical source can also be transmitted behind a diode or mirror. The movement of horizontal light does not interfere with a vertical light path. The number of tracks is assumed to be infinite in comparison to the small occupational dimensions of the components.

It is a considerable limitation on possible path assignments since light cannot pass through any of the components. To accommodate the possibility of assigning more than one diode to a single path, each diode occupation must be assigned to separate layers; otherwise, the light path will be conflicting as achieved by the constraint in Eq. (3.12). It

is only possible on the same layer to assign one diode or mirror on either side of the same track. As each layer adds depth to the side panel cost with tradeoff of sensitivity and touch penetration on a plane, the layer property can be determined or restricted depending on the goals of the design. The usage of layers is at most limited by the conflicting occupation of diodes and should not be exceeded, such that a compact and effective solution is obtained as reflected in the constraint in Eq. (3.13). Eq. (3.14) is a constraint to restrict all integers to be non-negative.

$$\text{Let } D_{ik} = \begin{cases} 1 & \text{if diode } i \text{ is assigned to layer } k \\ 0 & \text{otherwise.} \end{cases}$$

$$\text{Let } y_k = \begin{cases} 1 & \text{if any diode is assigned to layer } k \\ 0 & \text{otherwise.} \end{cases}$$

Let $n_L$ represent the number of total layers assigned.

Let $n_D$ represent the number of total diodes configured.

The Feasibility Model with predetermined values on $n_L$ and $n_D$:

$$s.t.\, a_{ij} \text{ uniqueness} \tag{3.11}$$

$$\sum_i a_{ij}\, D_{ik} = 1 \;\forall j, k \tag{3.12}$$

$$\sum_j a_{ij} \leq k \;\forall i \tag{3.13}$$

$$\text{All variables } \geq 0 \tag{3.14}$$

Since the most expensive component in the panel layout is diodes, the objective function in Eq. (3.15) is added to the feasibility model to determine the most economical solution by minimizing the number of diodes assigned.

$$\text{Min} \sum_i a_{ij} \tag{3.15}$$

Another variation of the model is examined to determine the minimal assignment of layers, as the design of the touch screen panel can be limited by space depth. In this variation, a new variable is defined to represent the number of layers and the objective function is modified.

A summary of the minimization of the layer model is presented as follows:

Let $m$ be an integer that represents the number of layers in the model

$$\text{Min } n_L \tag{3.16}$$

$$s.t.\, a_{ij} \text{ uniqueness} \tag{3.17}$$

$$m \geq \sum_i a_{ij} \ \forall j \tag{3.18}$$

$$\sum_i a_{ij}\, D_{ik} = 1 \ \forall j, k \tag{3.19}$$

$$\sum_j a_{ij} \leq k \ \forall i \tag{3.20}$$

$$\text{All variables } \geq 0 \tag{3.21}$$

An objective function that gives insight to the tradeoff in assigning an additional layer in favour of reduced diodes is evaluated. The tradeoff value ($\alpha$) is used in the objective function in Eq. (3.22). The sensitivity of the model to the value of $\alpha$ will give insight the precise weight of importance for design considerations.

$$\text{Min } \alpha\, n_d + n_L \tag{3.22}$$

## 3.6 CPLEX Implementation Constraints

The CPLEX solver cannot optimize variable dimension matrices. To fully solve the assignment of diodes and arrangement within the three dimensional space to optimality requires a single phase solution approach. The CPLEX implementation of the model requires the declaration of a larger zero entry matrix that is sufficiently large for the problem instance, effectively eliminating the requirement for variable matrix dimensions. Flags are then used

to identify which of the rows in the zero entry matrix are indeed assigned. For matrix $A$, to ensure that all appropriate assigned paths are included in the algorithm:

$$\text{Let } f_{A,i} \text{ denote the flag for matrix A on path } i \text{ be } \begin{cases} 1 & \text{if} \sum_j a_{ij} > 0 \\ 0 & \text{if} \sum_j a_{ij} = 0 \end{cases}$$

This is included in the formulation as the following constraints $(x)$:

Let $n_p$ denote the number of unique diode paths assigned in matrix $A$

$$\sum_j a_{ij} \leq n_p \times f_{A,i} \ \forall i \tag{3.23}$$

$$f_{A,i} \leq \sum_j a_{ij} \ \ \forall i \tag{3.24}$$

The dimensions of the layers matrix $D$ are also variable based on the dimensions of matrix $A$. Hence, a similar governing flag declaration is made to ensure that the total diodes on an overlapping layer does not exceed the maximum layer that may exist and the flag must be zero if the layer is not assigned. This constitutes the horizontal check on matrix $D$:

$$\text{Let } f_{D,i} \text{ denote the flag for matrix } D \text{ on path } i \text{ be } \begin{cases} 1 & \text{if} \sum_k D_{ik} > 0 \\ 0 & \text{if} \sum_k D_{ik} = 0 \end{cases}$$

$$\sum_k D_{ik} \leq L_{\max} \times f_{D,i} \ \forall i \tag{3.25}$$

$$f_{D,i} \leq \sum_k D_{ik} \ \ \forall i \tag{3.26}$$

where $L_{max}$ is the maximum layers assigned.

The vertical check on matrix $D$ ensures that the maximum number of diodes assigned on a layer does not exceed the maximum number of diodes assigned to each active layer. This is represented mathematically as:

$$\text{Let } L_k \text{ denote the flag for matrix } D \text{ be } \begin{cases} 1 & \text{if layer } k \text{ is assigned} \\ 0 & \text{otherwise} \end{cases}$$

$$\sum_i D_{ik} \leq N_{\max} \times L_k \ \forall k \tag{3.27}$$

$$L_k \leq \sum_i D_{ik} \ \forall k \tag{3.28}$$

where $N_{max}$ is the maximum number of diodes assigned.

The two sets of equations on matrix $A$ and $D$ also serve as rationality check on a logical solution and serves to tighten the search space of diode assignments to only active layers. The total number of assigned diodes in matrix $A$ and matrix $D$ must be equivalent:

$$f_{A,i} = f_{D,i} \ \forall i \tag{3.29}$$

## 3.7 Strengthened Model with Cuts

Constraints that reflect the framework allowances and violations are further added to tighten the search space in the model. In matrix $A$, an all zero assignment is not a unique code word assignment by the design criteria in Eq. (3.29). Also, the total number of diodes is greater or equivalent to the number of active layers used in the model is formulated in Eq. (3.30). The number of diodes assigned in matrix $A$ has an upper bound defined by the number of layers in use, represented by Eq. (3.3). The allowance that numerous diodes may be assigned to a single layer is enforced in Eq. (3.32). By framework design, Eq. (3.33) is the best possible lower bound solution and eliminates the solvers consideration of infeasible configurations.

$$\sum_i a_{ij} \leq n_l \forall j \tag{3.30}$$

$$n_d \geq n_l \tag{3.31}$$

$$\max_j \left( \sum_i a_{ij} = n_l \right) \tag{3.32}$$

$$\sum_i a_{ij} \leq n_l \, \forall j \tag{3.33}$$

$$\sum_i a_{ij} \geq \lfloor \log_2 (j) + 1 \rfloor \tag{3.34}$$

## 3.8 Symmetry Elimination

The branch and bound method is commonly used to solve integer programming problems. It effectively reduces the feasible solutions into partitioned sets to form easily solved sub-problems. However, the possible permutations of a diode assigned to a certain layer and a diode to a certain path introduces a significantly large search space for such a heavily symmetric problem. The solver will partition many of the same sub-problems due to the symmetric nature of the problem, when only a single collection of equivalent sub-problems need to be solved. While symmetry cannot be omitted or reformulated in the model, it can be reduced significantly using symmetry breaking techniques [49]. The symmetry breaking approach in the model dictates the assignment of diodes to paths in decreasing numbers demonstrated when Eq. (3.35)-(3.38) are applied to the $A$ and $D$ matrices. This method eliminates permuted solutions that are either mirrored forms or order shuffled by layers.

$$\sum_{j} a_{i,j} \leq \sum_{j} a_{i-1,j} \ \forall i \in \{1, ..., (D_{\max} - 1)\} \tag{3.35}$$

$$\sum_{i} a_{i,j} \leq \sum_{i} a_{i,j-1} \ \forall j \in \{1, ..., (n_p - 1)\} \tag{3.36}$$

$$\sum_{k} D_{i,k} \leq \sum_{k} D_{i-1,k} \ \forall i \in \{1, ..., (D_{\max} - 1)\} \tag{3.37}$$

$$\sum_{i} D_{i,k} \leq \sum_{i} D_{i,k-1} \ \forall k \in \{1, ..., (L_{\max} - 1)\} \tag{3.38}$$

## 3.9 Comprehensive Formulation

By using the inspirational assignment declaration of CGT and superimposed codes to significantly reduce the representation of a larger subset of data to the diodes-paths assignment, the problem is fully capture in the defined framework implementation in this chapter. Performance enhancements in variable dimension optimization, model cuts strengthening, and symmetry breaking were also required to enforce the model for reasonable runtime.

The complete model formulation is the inclusion of constraints Eq. (3.18)-(3.21), and (3.23)-(3.38) with the XOR uniqueness constraints of either Eq. (3.3)-(3.6) or Eq. (3.7)-(3.10) and an objective function of Eq. (3.15) for diode minimization, Eq. (3.16) for layer reduction, or Eq. (3.22) for trade-off evaluations.

# Chapter 4

# Model Results and Analysis

The model formulation presented in Chapter 3 was implemented in CPLEX version 11.100 and the results are presented in this chapter. The first evaluation was the performance of the XOR code to determine which of the three methods had the least runtime. The feasibility model, minimization of diodes, and reduction focus on layers were investigated by varying the objective function. To gain a better understanding of the relationship between the number of assigned diodes and available layers, a trade-off comparison was completed. As a preliminary investigation in the reduction of signal representation for electronic devices, the concluded analysis gives insight to the direction of future developments.

## 4.1 XOR Performance

In the formulation of the uniqueness constraint, three methods of XOR code are examined. It is essential for the XOR comparison to execute in an effective time frame as it will be scaled by the dimension of the problem instances. The execution of the model formulation depends heavily on the runtime performance of the XOR comparison function.

The performance of the XOR function in linear representation, array representation, and built-in CPLEX function are given for various matrix dimensions in Table 4.1. The CPLEX function performed exceptionally slow and the implementation methods were unclear, thus making it difficult to enhance the runtime performance. Although it is expected that the linear representation perform favourable, given the group of equations simplicity, the equations were not able to effectively eliminate cliques and was cumbersome in the

repetitive evaluations set. In contrast, the array representation had superior performance and efficiency in large sized problems. The array structure exploited the individual component evaluations without repeatedly comparing the same values. In the research model evaluation, the array representation of XOR uniqueness comparison was used.

Table 4.1: Performance comparison of XOR implementations.

| Resolution Dimension | | Runtime (s) | | |
|---|---|---|---|---|
| #Path | Assign. Diode | Built in XOR | Linear XOR | Array XOR |
| 5 | 3 | 0.05 | 0.16 | 0.04 |
| 10 | 4 | 73.76 | 0.57 | 0.23 |
| 15 | 4 | 502.25 | 298.94 | 3.29 |
| 20 | 5 | 1405.63 | 401.38 | 5.46 |
| 25 | 5 | 2345.29 | 572.64 | 8.84 |
| 30 | 5 | 3902.13 | 720.51 | 10.54 |
| 35 | 7 | 5028.32 | 901.69 | 13.69 |

## 4.2 Feasibility Model Results

The feasibility model is evaluated without an objective function and the primary goal is to determine a possible solution given a specific number of diodes and layers. The results are summarized in Table 4.2, where the model optimally solved three instance sized 5, 10, and 20 with equally assigned diodes and layers. The model has greater difficulty in assigning uneven number of diodes and layers because the trade-off cost is not specifically assigned in the objective function. In the instance of 15 paths, the problem may be subjected to a higher degree of symmetry and does not solve after an extended time frame. For 25 paths, the problem solves to a gap of 16.67%, which is the assignment of one additional diode than the theoretical limit. It is important to realize that the theoretical limit does not consider touch panel limitations and requirements.

## 4.3 Independent Minimizing Model Results

The results for the minimization of the total number of assigned diodes are summarized in Table 4.3. The model obtained the theoretical lower bound on the resolution paths for 5, 10, 15, 20, and 30. Although the possible existing solutions are greater for smaller dimension problems, the model displays difficulty in eliminating the additional diode assignment

Table 4.2: Performance for determining feasibility.

| Instance | | Feasibility Specified by Path | | Performance | | | |
|---|---|---|---|---|---|---|---|
| #Path | Theor. Diode | Assign. Diode | Layers | Runtime (s) | Nodes | Iterations | Gap % |
| 5 | 3 | 3 | 2 | 0.17 | 0 | 0 | 0.00 |
| 10 | 4 | 4 | 4 | 0.20 | 0 | 0 | 0.00 |
| 10 | 4 | | 3 | Unsolved after 11272.60 | | | |
| 15 | 4 | | 4 | Unsolved after 21023.95 | | | |
| 20 | 5 | 5 | 5 | 2.33 | 0 | 375 | 0.00 |
| 25 | 5 | 6 | 6 | 3582.69 | 145300 | 4508382 | 16.67 |
| 100 | 7 | 8 | 5 | Unsolved after 33620.37 | | | |

in resolution paths of 25, 35, 40, 45, and 50. The time and solver details when the lowest gap is first found is provided for all problems that did not solve to optimality within a reasonable timeframe. In larger sized resolutions of 100 and 150 diode paths, it is very difficult to determine unique paths and achieve the theoretical limit. However, the theoretical limit, which is the information lower bound, does not account for touch panel requirements and the reduction of 100 signal detection to just 10 is a significant accomplishment. The resolution path of 200 exceeds the CPLEX program memory allocation and gives insight to the substantial dimension of the overall problem.

The computation of minimizing the overall assigned layers results are shown in Table 4.4. The objective function uses Eq. (3.16) with the remainder of the model unchanged. The results for small dimensions of 5 and 10 paths are solved by assigning a single diode to each resolution path on one layer. The model does not provide enough tight constraints on the trade-off between layers assigned in this regard. In the 15 and 20 dimensions, since the model cannot assign a diode per layer, it has greater difficulty determining the ideal configuration.

The minimization of total assigned layers is purely empirical when in reality, the numbers of available layers for assignment are predetermined. The cost of expanding the touch panel depth would be seen as more expensive in implementation and execution as it limits the sensitivity of user touch operation. It is still in the interest of the design to use diodes before expanding the number of available layers.

Table 4.3: Minimizing Diodes Assigned Computational Results.

| Instance | | Assigned Solution | | Performance | | | | | | | |
|---|---|---|---|---|---|---|---|---|---|---|---|
| #Path | Theor. Diode | Diodes | Layers | Runtime (s) | Nodes | Iterations | Gap % | Reached Gap (s) | Nodes | Iteration | # Sol. |
| 5 | 3 | 3 | 2 | 0.17 | 4 | 90 | 0.00 | | | | |
| 10 | 4 | 4 | 4 | 0.86 | 146 | 1228 | 0.00 | | | | |
| 15 | 4 | 4 | 4 | 14.39 | 2180 | 60240 | 0.00 | | | | |
| 20 | 5 | 5 | 5 | 17.41 | 1513 | 24303 | 0.00 | | | | |
| 25 | 5 | 6 | | 14408.02 | 889900 | 39754480 | 16.67 | 145.34 | 9390 | 186822 | 5 |
| 30 | 5 | 5 | 5 | 1114.20 | 50932 | 2427501 | 0.00 | | | | |
| 35 | 6 | 7 | | 10556.17 | 395600 | 18756023 | 14.29 | 131.50 | 4290 | 925006 | 4 |
| 40 | 6 | 7 | | 10576.42 | 307600 | 6023676 | 14.29 | 290.75 | 2955 | 32431 | 4 |
| 45 | 6 | 7 | | 5657.80 | 97000 | 4732273 | 14.29 | 315.16 | 6320 | 131709 | 4 |
| 50 | 6 | 7 | | 7339.11 | 25100 | 1657966 | 14.29 | 587.81 | 3000 | 75575 | 4 |
| 100 | 7 | 10 | | 7679.65 | 10400 | 255314 | 30.00 | 160.15 | 100 | 7892 | 1 |
| 150 | 8 | 8 | | Unsolved | | | | 5443.22 | 2 | 14611 | 1 |
| 200 | 8 | 8 | | Out of memory | | | | | | | |

Table 4.4: Computation results for minimized number of assigned layers.

| Instance | | Assigned Solution | | Performance | | | | |
|---|---|---|---|---|---|---|---|---|
| #Path | Theor. Diode | Diodes | Layers | Runtime (s) | Nodes | Iterations | Gap % | # Sol. |
| 5 | 3 | 5 | 1 | 0.20 | 2 | 224 | 0.00 | |
| 10 | 4 | 10 | 1 | 0.09 | 1 | 110 | 0.00 | |
| 15 | 4 | | 2 | 22559.88 | 5011000 | 94550096 | 50.00 | 3 |
| 20 | 5 | | 1 | 27372.30 | 7891030 | 131984503 | 50.00 | 5 |

## 4.4 Assignment Solution Analysis

Each solution generates a different configuration and permutations are possible by swapping layers or mirroring the assignment of diodes vertically. For the five path resolution problem, considering the minimization of total number of diodes resulted in the use of three diodes committed to two layers in the resulting configurations summarized in Table 4.5. Diode zero starts at path 0 and is reflected down through paths 1 and 2. Diode one traverses paths 1 and 3, while diode two navigates line 0 and line 4. Due to the overlap on line 1, two layers are necessary. Any touch detection at any of the resolution lines will result in a uniquely identifiable localization.

Table 4.5: Optimal configuration for five resolutions.

| | Path | | | | | | Layer | | | | | | | | | | |
|---|---|---|---|---|---|---|---|---|---|---|---|---|---|---|---|---|---|
| Diode | 0 | 1 | 2 | 3 | 4 | | Diode | 0 | 1 | 2 | 3 | 4 | 5 | 6 | 7 | 8 | 9 | Layer # |
| 0: | 1 | 1 | 1 | 0 | 0 | | 0: | 0 | 1 | 0 | 0 | 0 | 0 | 0 | 0 | 0 | 0 | 1 |
| 1: | 0 | 1 | 0 | 1 | 0 | | 1: | 1 | 0 | 0 | 0 | 0 | 0 | 0 | 0 | 0 | 0 | 0 |
| 2: | 1 | 0 | 0 | 0 | 1 | | 2: | 1 | 0 | 0 | 0 | 0 | 0 | 0 | 0 | 0 | 0 | 0 |
| Total Diodes: 3 | | | | | | | Total Assigned Layers: 2 | | | | | | | | | | | |

## 4.5 Trade-off Minimizing Diodes and Layers

To fully understand the trade-off between minimizing diodes and layers, a varied factor of $\alpha$ is introduced in the objective function. From the previous model evaluation and results,

the cost of expanding the number of diode assigned is less than the trade-off of an additional layer. Hence, $\alpha$ is increased in intervals of 0.2 from 0.1 to 0.9. The computational results are shown in Table 4.6. The optimal solution was found for an instance of resolution path 5 using 5 diodes on one layer with the runtime increasing as $\alpha$ increased. When the diode weight became comparable to the layer assignment at values of 0.7 and 0.9, the diode assigned decreased to 3 on 2 layers. Hence, the trade-off for lower diodes in favor of increased layers occurs at $\alpha = 0.5$ and $\alpha = 0.7$. The gap percentage from optimality increases for the 5 and 10 path instance but in general, decreases with the increased alpha values.

Gaps in the model assignment are apparent in all greater path resolutions. The results indicate the time when the smallest gap was found before timing out at 1800 seconds. For larger $\alpha$, the solver was able to eliminate a greater set of constraints. The smallest gap was found when $\alpha = 0.9$, with the model even solving an instance of 200 paths when all other factors resulted in an out of memory error. The reduction of sensors required by dimension is greatly reduced in the model formulation. Despite gap existence, it is possible to use the minimally additional diodes to achieve a significantly reduced assignment of sensors in the touch screen. The most notable being of instance 100 resolution paths that 11 sensor-diode pairs can cover the same space as a 100 signal input. The resolution path causes the growth in $A$ matrix dimensions and coincidentally the $D$ matrix grows accordingly, which can slow the overall ability of the model to solve within a reasonable amount of time.

## 4.6 Research Model Analysis

The research model solves to optimality for 5 resolution paths in all formulation variations. The runtime and performance prove that the reduction of signals can be applied to any touch screen design as a reduction factor of five, allowing five resolution paths to be grouped as a single set of input. Determining additional reductions in problem formulation would exceed the capabilities of the research model to achieve the theoretical lower bound, and other techniques need to be investigated. Although the overall problem reduction benefits were not immediately applicable for all larger dimensions, the findings can be scaled to a series of resolution lines such that noteworthy reduction in signal processing can be achieved. Even at higher resolution paths, while the model may not achieve the theoretical

Table 4.6: Varying $\alpha$ trade-off results of minimizing diodes and layers assignment.

| Instance | | $\alpha = 0.1$ | | | $\alpha = 0.3$ | | | $\alpha = 0.5$ | | | $\alpha = 0.7$ | | | $\alpha = 0.9$ | | |
|---|---|---|---|---|---|---|---|---|---|---|---|---|---|---|---|---|
| #Path | Theor. Diodes | Runtime (s) | Gap (%) | # Sol. | Runtime (s) | Gap (%) | # Sol. | Runtime (s) | Gap (%) | # Sol. | Runtime (s) | Gap (%) | # Sol. | Runtime (s) | Gap (%) | # Sol. |
| 5 | 3 | 1.25 | 0.00 | 5D on 1L | 1.29 | 0.00 | 5D on 1L | 2.34 | 0.00 | 5D on 1L | 2.65 | 0.00 | 3D on 2L | 2.59 | 0.00 | 3D on 2L |
| 10 | 4 | 1105.18 | 10.00 | 5 | 302.54 | 8.57 | 7 | 245.1 | 11.11 | 5 | 179.27 | 12.73 | 5 | 103.06 | 13.85 | 5 |
| 15 | 4 | 1016.11 | 38.46 | 5 | 1654.61 | 26.46 | 12 | 811.39 | 20.00 | 7 | 2495.30 | 22.58 | 5 | 1974.00 | 25.68 | 3 |
| 20 | 5 | 821.47 | 80.77 | 4 | 1666.04 | 56.90 | 7 | 97.13 | 50.00 | 4 | 971.22 | 51.09 | 7 | 1192.23 | 40.86 | 5 |
| 25 | 5 | 1949.69 | 61.54 | 7 | 792.53 | 63.24 | 6 | 1674.13 | 63.16 | 5 | 1205.71 | 61.21 | 5 | 183.78 | 51.75 | 2 |
| 30 | 5 | 1496.08 | 77.61 | 6 | 696.60 | 70.24 | 4 | 836.55 | 69.57 | 4 | 1490.33 | 55.88 | 6 | 591.32 | 58.65 | 3 |
| 35 | 6 | 630.52 | 83.84 | 3 | 1203.17 | 74.55 | 3 | 746.87 | 66.67 | 4 | 288.89 | 67.5 | 2 | 575.49 | 60.25 | 3 |
| 40 | 6 | 620.77 | 83.84 | 3 | 45.62 | 78.46 | 1 | 972.09 | 69.23 | 3 | 729.79 | 61.76 | 2 | 1093.38 | 51.88 | 2 |
| 45 | 6 | 18.05 | 85.45 | 1 | 1118.57 | 76.67 | 2 | 21.27 | 73.33 | 1 | 234.24 | 67.50 | 2 | 899.69 | 51.88 | 3 |
| 50 | 6 | 17.10 | 85.45 | 1 | 1434.71 | 76.07 | 2 | 789.91 | 70.37 | 2 | 38.01 | 69.41 | 1 | 927.34 | 62.57 | 2 |
| 100 | 7 | 280.18 | 84.55 | 1 | 289.96 | 76.15 | 1 | 174.42 | 70.00 | 1 | 175.01 | 65.29 | 1 | 289.13 | 61.58 | 1 |
| 200 | 8 | Out of Memory | | | Out of Memory | | | Out of Memory | | | Out of Memory | | | 1790.56 | 56.84 | 1 |

information theory lower limit, it only requires an additional one to three diodes. The trade-off value for an additional layer in favour of decreased diode occurs at $\alpha = 0.5$ and $\alpha = 0.7$.

The model results are for single touch detection along a single axis. The performance is considered to occur in parallel time for detection in two dimensions without interference. The resulted assignment can be duplicated for the other axis but an additional controller is required to process the data. The model can still achieve favourable reduction for multi-touch control. However, the performance runtime still indicates that the problem needs additional modification to solve within an acceptable timeframe.

The difficulty of the problem remains with the uniqueness constraint and the arrangement of paths. The symmetry in the problem inherent with combinatorial and permuted instances severely hinder the solution performance time. A direct result of this research model is the capability to model a three dimensional assignment and arrangement of diodes with varying dimensions. Solutions of the model provide sufficient background for further implementation enhancements.

# Chapter 5

# Conclusive Remarks and Future Work

Despite the rapidly growing industry of touch screen technology deployment, scarce improvements to the design of signal reduction have been made. In this thesis, significant signal reduction was proposed through the incorporation of combinatorial group theory and superimposed codes to structure the assignment matrix. Through the linear optimization of the NP-complete problem, computational results were evaluated and investigated to further provide insight into the problem nature. The array representation of the XOR function and aggressive symmetry breaking constraints are necessary for the research formulation to solve and provide efficient runtime.

The research model depicted a minimally assigned diode solution for up to 30 resolution paths with the exception of dimension 25, while the sensitivity of an additional layer in favour of diode reduction is detected at the trade-off $\alpha$ parameter between 0.5 and 0.7. The computational analysis show that an overall reduction by a factor of five is optimally possible to the theoretical information theory bound within seconds. For instance of 30 through to 100, the theoretical lower bound was not achieved but in general, required one to three additional diodes, which is still a momentous reduction. The empirical data indicate that for larger resolution paths, additional reduction techniques need to be employed for acceptable performance runtimes.

As a novel approach to signal reduction, the results provided a foundation for future investigations and enhancements. One such notable area is the implementation of grey-

codes, which is a coding structure that can be used as an extension beyond the five code word basis. Additionally, in the model framework, the path structure is limited to vertical and horizontal transmission of light as reflected by right angles. Future research models can consider the reflection of light on any angle, allowing greater freedom of optimization over three dimensional space while offering more unique paths. The location of components can also be varied in configuration. While the use of components with different properties were not considered, such as diodes on different wavelengths and mirrors with partial reflection, the introduction of these factors would provide further design flexibility.

# Bibliography


[1] C. Forlines et al, "Direct-Touch vs. Mouse Input for Tabletop Displays," *CHI 2007 Proc. Mobile Interaction Techniques I*, Apr 2007.

[2] S. Khatri, "Touch Screen Interfaces Driving Growth in Signage and Professional Markets," *Emerging Display Technologies Q4 iSuppli*, 2009.

[3] I. Sutherland, "A man-machine graphical communications systems," *Proc. Spring Joint Computer Conference*, pp. 429-346, 1963.

[4] D. Engelbart and W. English, "Research Center for Augmenting Human Intellect," *AFIPS Conference Proc. Fall Joint Computer Conference*, vol. 33, pp. 395-410, 1968.

[5] D. Wang, K. Tuer, M. Rossi and J. Shu, "Haptic Overlay Device for Flat Panel Touch Displays," *IEEE Proc. 12th International Symposium on Haptic Interfaces for Virtual Environment and Teleoperator Systems*, 2004.

[6] I. Poupyrev, S. Maruyama, and J. Rekimoto, "Ambient Touch: Designing Tactile Interfaces for Handheld Devices," *CHI UIST*, vol. 4, pp. 51-60, Oct. 2002.

[7] R. H. Hartson, H.R. Hartson, and D. Hix, "Advances in Human-Computer Interaction," Volume 3, *Norwood: Ablex Publishing Corporation*, 1992.

[8] J. Y. Han, "Low-Cost Multi-Touch Sensing through Frustrated Total Internal Reflection," *Proc. 18th Annual ACM Symp. User Interface Software and Technology*, 2005.

[9] B. Ullmer, and H. Ishii, "The metaDESK: Models and Prototypes for Tangible User Interfaces," *ACM Symposium on USIT*, pp. 223-232., 1997

[10] N. Matsushita, J. Rekimoto, "HoloWall: Designing a Finger, Hand, Body and Object Sensitive Wall," *ACM Symposium on UIST*, 1997.

[11] S.R. Klemmer, et al, "The Designer's Output: A Tangible Interface for Collaborative Web Site Design," *ACM Symposium on User Interface Software and Technology,* pp.1-10., 2001.

[12] S. Hotelling, J. A. Strickon, and B. Q. Huppl, "Multipoint Touchscreen," *U. S. Patent 9,7991*, May 11, 2006.

[13] S. P. Hotelling et al, "Touch Screen Liquid Crystal Display," *U. S. Patent 62,148*, Mar. 13, 2008.

[14] S. Lee, W. Buxton, and K.C. Smith, "A Multi-Touch three Dimensional Touch-Sensitive Tablet," *SIGCHI ACM,* pp.21-25., Apr. 1985.

[15] P. Dietz, and D. Leigh, "DiamondTouch: A Multi-User Touch Technology," *UIST ACM Press*, pp.219-226., Nov. 2001.

[16] J. Rekimoto, "SmartSkin: An Infrastructure for Freehand Manipulation on interactive Surfaces," *SIGCHI ACM,* pp.113-120., Apr. 2002.

[17] S. Izadi, et al, "ThinSight: Integrated Optical Multi-Touch Sensing through Thin Form-Factor Displays," *Proc. 2007 workshop on Emerging Displays Technologies*, 2007.

[18] S. Hotelling, "Mutual Capacitance Touch Sensing Device," *U.S. Patent 7,539,* Jan. 10, 2008.

[19] M. Csele, *Fundamentals of Light Sources and Lasers,* Hoboken, Wiley-Interscience, 2004.

[20] S.L. Chin, *Fundamentals of Laser Optoelectronics,* Teaneck, World Scientific, 1989.

[21] D. Z. Du and F. K. Hwang, *Combinatorial Group Testing and Its Applications,* 2nd ed, Applied Mathematics Vol. 12. River Edge: World Scientific Publishing Company, 2000.

[22] R. W. Hamming, "Error Detecting and Error Correcting Codes," *The Bell System Technical Journal,* Vol. 26, No. 2, April 1950, pp.147-160.

[23] W. W. Peterson, *Error-Correcting Codes,* MIT Press, 1961.

[24] M. Sobel and P. A. Groll, "Group Testing to Eliminate Efficiently All Defectives in a Binomial Sample," *Bell Syst. Tech. J.,* vol. 38, pp. 1179-1252, 1959.

[25] W. H. Kautz and R. C. Singleton, "Nonrandom binary Superimposed Codes," *IEEE Trans. Inform. Theory,* vol. 10, pp. 363-377, Oct 1964.

[26] C. H. Li, "A sequential method for screening experimental variables," *J. Amer. Stat. Assoc.,* vol. 57, pp. 455-477, 1962.

[27] T. Berger, N. Mehravari, D. Towsley, and J. Wolf, "Random multiple- access communication and group testing," *IEEE Trans. Commun.,* vol. 32, pp. 769-779, 1984.

[28] M. Xie, K. Tatsuoka, J. Sacks, and S. S. Young, "Group testing with blockers and synergism," *J. Amer. Stat. Assoc.,* vol. 96, pp. 92-102, 2001.

[29] E. H. Hong and R. E. Ladner, "Group testing for image compression," *IEEE Trans. Image Process.,* vol. 11, pp. 901-911, 2002.

[30] E. Hong, R. E. Ladner, and E. A. Riskin, "Group testing for image compression using alternative transforms," *Signal Process.: Image Commun.,* vol. 18, pp. 561-574, 2003.

[31] G. Cormode and S. Muthukrishnan, "What's hot and what's not: Tracking most frequent items dynamically," *ACM Trans. Database Syst.,* vol. 30, no. 1, pp. 249-278, 2005.

[32] *Envirom. Ecological Stat.: Special Issue on Composite Sampling,* vol. 8, pp. 89-180, 2001.

[33] E. Barillot, B. Lacroix, and D. Cohen, "Theoretical analysis of library screening using an N-dimensional pooling strategy," *Nucl. Acids Res.,* pp. 6241-6247, 1991.

[34] D. Margaritis and S. Skiena, "Reconstructing strings from substrings in rounds," *Proc. Found. Comput. Sci. (FOCS 95),* pp. 613-620, 1995.

[35] Y. Cheng, D. Z. Du, K. I. Ko, and G. Lin, "On the Parameterized Complexity of Pooling Design," *Journal of Computational Biology,* vol. 16, pp. 1529-1537, 2009.

[36] W. H. Kautz and R. C. Singleton, "Nonrandom binary Superimposed Codes," *IEEE Trans. Inform. Theory,* vol. 10, pp. 363-377, Oct 1964.

[37] F. K. Hwang, T. T. Song, and D. Z. Du, "Hypergeometric and Generalized Hypergeometric Group Testing," *SIAM J. Alg. Dis. Methods,* vol. 2, pp. 426-428, Dec. 1981.

[38] A. D'yachkov, A. Macula, and V. V. Rykov, "New Constructions of Superimposed Codes," *IEEE Trans. Inform. Theory,* vol. 46, no. 1, pp. 284-290, Jan. 2000.

[39] D. R. Stinson, R. Wei, and L. Zhu, "New Constructions for Perfect Hash Families and RelatedStructures Using Combinatorial Designs and Codes," *J. Combin. Des.,* vol. 8, no. 3, pp. 189-200, 2000.

[40] G. Cohen, S. Encheva, and S. Litsyn, "Intersecting Codes and Identifying Codes," *WCC2001 Int. Workshop on Coding and Cryptography,* vol.6, pp. 211-219, April 2001.

[41] K. A. S. Quinn, "Bounds for Key Distribution Patterns," *J. Cryptology,* vol. 12, no. 4, pp. 227-239, Dec. 1999.

[42] B. Chor, A. Fiat, M. Naor, and B. Pinkas, "Tracing Traitors," *IEEE Trans. Inform. Theory,* vol. 46 no. 3, pp. 893-910, 2000.

[43] A. De Bonis and U. Vaccaro, "Optimal Algorithms for Two Group Testing Problems, and New Bounds on Generalized Superimposed Codes," *IEEE Trans. Inform. Theory,* vol. 52 no.10, pp.4673-4680, Oct. 2006.

[44] S. Hong, S. Kapralov, H.K. Kim, and D. Y. Oh, "Uniqueness of some Optimal Superimposed Codes," *Problems of Information Transmission,* vol. 43, pp 113-123, 2007.

[45] S. M. Sinha, *Mathematical Programming: Theory and Methods,* Delhi: Elsevier, 2006.

[46] M. S. Bazaraa, J. J. Jarvis, and H. D. Sherali, *Linear Programming and Network Flows,* 4th ed, Hoboken: John Wiley & Sons, 2010.

[47] F. K. Hwang, T. T. Song, and D. Z. Du, "Hypergeometric and Generalized Hypergeometric Group Testing" *SIAM J. Alg. Dis. Methods,* vol. 2, pp. 426-428, Dec. 1981.

[48] B. Wu, P. H. Ho, and K. Yeung, "Monitoring Trail: a New Paradigm for Fast Link Failure Localization in WDM Mesh Networks," *GLOBECOM- IEEE Global Telecommunications Conference*, pp 2709-2713, 2008.

[49] J. Ostrowski, "Symmetry in Integer Programming," *Ph.D. dissertation, Lehigh University,* Bethlehem, PA, United States of America, 2008.